

Tunable oleosome-based oleogels: Effect of polysaccharide architecture on polymer bridging-based structuring

Cite as: Phys. Fluids **35**, 027131 (2023); <https://doi.org/10.1063/5.0138206>

Submitted: 09 December 2022 • Accepted: 02 February 2023 • Accepted Manuscript Online: 03 February 2023 • Published Online: 24 February 2023

 Juan C. Zambrano and  Thomas A. Vilgis

COLLECTIONS

Paper published as part of the special topic on [Special Issue on Food Physics](#)

 This paper was selected as an Editor's Pick



View Online



Export Citation



CrossMark

ARTICLES YOU MAY BE INTERESTED IN

[The interactions of the elliptical instability and convection](#)

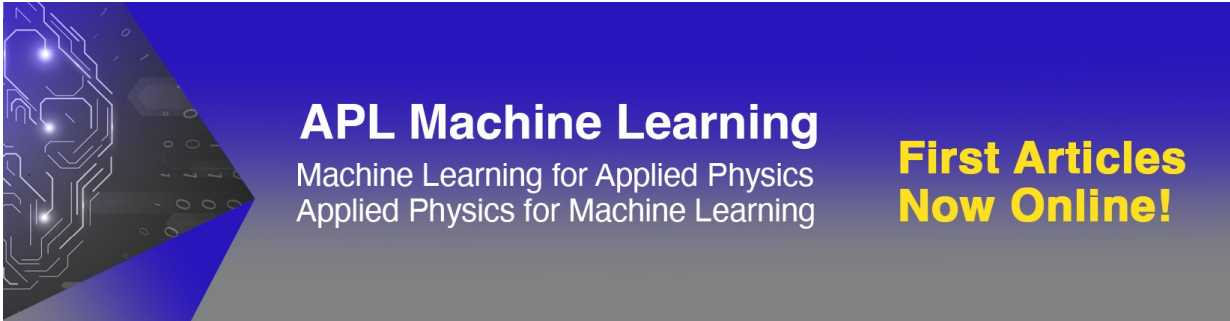
Phys. Fluids **35**, 024116 (2023); <https://doi.org/10.1063/5.0135932>

[Multi-scale analysis of solute dispersion in non-Newtonian flows in a tube with wall absorption](#)

Phys. Fluids **35**, 033103 (2023); <https://doi.org/10.1063/5.0130789>

[Experimental and numerical investigation of beer foam](#)

Phys. Fluids **35**, 023318 (2023); <https://doi.org/10.1063/5.0132657>



APL Machine Learning
Machine Learning for Applied Physics
Applied Physics for Machine Learning

**First Articles
Now Online!**

Tunable oleosome-based oleogels: Effect of polysaccharide architecture on polymer bridging-based structuring

Cite as: Phys. Fluids **35**, 027131 (2023); doi: 10.1063/5.0138206
Submitted: 9 December 2022 · Accepted: 2 February 2023 ·
Published Online: 24 February 2023



View Online



Export Citation



CrossMark

Juan C. Zambrano^{a)}  and Thomas A. Vilgis^{a)} 

AFFILIATIONS

Max Planck Institute for Polymer Research, Ackermannweg 10, 55128 Mainz, Germany

Note: This paper is part of the special topic, Special Issue on Food Physics.

^{a)}Authors to whom correspondence should be addressed: zambrano@mpip-mainz.mpg.de and vilgis@mpip-mainz.mpg.de

ABSTRACT

A simple method for structuring natural oleosome emulsions by polymer-bridging mechanism is proposed. Polymer bridging of oleosome droplets was induced by the addition of two different adsorbing polymers. Over a range of polymer/oleosome ratios, the mixture results in the formation of a particle gel network of aggregated oleosome droplets. It is found that polymer bridging ability is heavily influenced by the strength of binding between polymer and oleosome surface where sodium alginate interacted stronger to oleosome surface than *l*-carrageenan. These effects are associated with the different molecular architecture and physical differences between the two hydrocolloids. Alginate has a co-block arrangement of charged and uncharged units. The polymer promotes stronger adsorption to the oleosome surface, in contrast to *l*-carrageenan, where the negative charges are distributed uniformly along its chain. The polymer bridging ability will influence the resulting microstructure and therefore rheological properties. Confocal scanning laser microscopy showed that the difference in microstructure is mainly in the extent of heterogeneity over different length scales where sodium alginate produced the most heterogeneous microstructures. Bridging-flocculated emulsions showed power-law scaling behavior of the storage modulus with the oleosome concentration, which was explained using percolation theory.

© 2023 Author(s). All article content, except where otherwise noted, is licensed under a Creative Commons Attribution (CC BY) license (<http://creativecommons.org/licenses/by/4.0/>). <https://doi.org/10.1063/5.0138206>

I. INTRODUCTION

Food emulsions are ubiquitous in many products, such as soft drinks, spreads, and ice cream. The oil droplets in emulsions significantly affect sensory perception of o/w emulsion-based foods since they provide, for instance, thickness and creaminess perceptions (de Wijk *et al.*, 2011; Upadhyay *et al.*, 2020). Since rheological properties mainly define sensorial perceptions of o/w emulsions, it is interesting to expand the range of viscoelastic properties of emulsions. The benefits are manifold and include a broader range of possibilities in applications in the food industry, e.g., reduced-fat food products and novel formulations for non-animal-based foods. Gelation of food emulsions may result in the formation of distinct textures and can also be designed to control the release of flavor compounds by entrapping them into the oil droplets.

Using natural emulsions based on oil bodies, or so-called oleosomes, stands as an alternative to conventional methods for emulsion

preparation. Oleosomes are natural particles that exist in oleaginous seeds already as pre-emulsified oil droplets. Extracted oleosomes benefit from environmentally friendly methods because they require gentle extraction by using water as the solvent medium instead of conventional oil-extracting organic solvents, such as hexane. This is also relevant to health concerns. Moreover, aqueous extraction yields oleosome particles with remarkable physical stability and sizes ranging from the nanoscale to a few μm (Tzen *et al.*, 1993), depending on the botanical origin.

From a soft matter point of view, emulsions are colloidal dispersions that can be assembled to create new colloidal structures, which may directly impact macroscopic properties such as texture (Vilgis, 2013). Emulsion self-assembly can be done, for instance, by the modification of its surface properties that are given by a certain balance between repulsive and attractive forces. By manipulating these interparticle forces, the destabilization of an emulsion can lead to droplet

aggregation, which modifies the rheological behavior of emulsions from viscous liquids to semi-solid products (Dickinson, 2019). In conventional emulsions, it is essential to control the aggregation of oil droplets to create products with defined rheological properties. Several approaches have been previously accomplished on the controlled aggregation of emulsions: (1) *reduction of electrostatic repulsion* in protein-stabilized oil droplets by altering the pH or ionic strength to reduce the charge on the droplets (Patel *et al.*, 2019); (2) *aggregation due to attractive hydrophobic interactions* in protein-stabilized droplets due to the effect of high temperatures on the structural conformation of globular proteins (Dickinson and Parkinson, 2004); (3) *enzymatic induced aggregation* by either removing sections of the peptide chain of the proteins that lead to a reduction of steric hindrance or crosslinks between protein-stabilized oil droplets (Fuhrmann *et al.*, 2019; Lee *et al.*, 2006); (4) *hetero-aggregation of emulsion droplets* when two or more oppositely charged emulsions varying in droplet size, concentration, or charge density are mixed, and by the effect of electrostatic attractions, the result is the formation of micro-clusters of different rheological properties depending on the interaction strength between the oil droplets (Mao and McClements, 2012; Wang *et al.*, 2019); (5) *aggregation by complexation of polyphenols molecules*, e.g., *proanthocyanidins with protein-stabilized oil droplets*, produces cross-linking of oil droplets as an effect of a broad range of specific interactions such as hydrogen bonds, hydrophobic interactions, π - π stacking, and covalent bonds (Fuhrmann *et al.*, 2020).

Adding polysaccharides to colloidal dispersions is another effective method to control the assembly of emulsion droplets. Particles aggregate through polymer bridging if an adsorptive polysaccharide is added at concentrations below particle total surface coverage. Polymer bridging flocculation is a well-known mechanism in colloid science. It occurs when a polymer chain adsorbs on two or more particles, and attractive interactions mediate between the polymer and the particle surface, which is often electrostatic origin and of the order of hundred $k_B T$. As a result, a particle network is formed with relatively strong and irreversible bonds. Due to this, bridging-flocculated particle network can be exploited to design semi-soft materials that can have great flexibility to alter rheological properties. Zhao *et al.* previously showed the gelation of microspheres through a bridging mechanism induced by microgels (Zhao *et al.*, 2012). However, bridging flocculation has received little attention as a gelation mechanism in food emulsions. Although studies have shown emulsions gelled by bridging flocculation produce strong gel networks (Blijdenstein *et al.*, 2004a), bridging flocculation has been referred to mainly as an instability phenomenon affecting emulsions' shelf life (Dickinson, 2019; Zhai *et al.*, 2021).

Nevertheless, polymer bridging is a promising alternative to tailor the rheological properties of oleosomes as natural templates. Previously (Zambrano and Vilgis, 2023), it was shown that polysaccharide concentrations as low as 0.025 wt. % could produce compact self-supporting gels from oleosome concentrations of 5 wt. %. Oleosomes are covered by a unique monolayer composed of phospholipids connected to a particular protein called oleosin. These proteins are unique because they have a long hydrophobic domain that is partly in contact with the oil core while deeply trapped within the phospholipids layer. The outer part of the protein is made of two amphipathic N- and C-terminals that protrude toward the aqueous phase and provide electrical charge characteristics. This charged nature of oleosomes allows them to adsorb onto their surface, charged polysaccharides

from different characteristics, providing an opportunity to influence aggregation and design droplet networks with different structures and properties.

However, obtaining control over network formation is challenging. In polymer bridging flocculation, aggregate formation is determined by the interplay between the configuration properties of the polymer chains, the concentration of free polymer in the continuous phase, and the volume fraction of particles. An earlier publication (Zambrano and Vilgis, 2023) showed that optimum bridging occurs at a certain ratio between the polymer content and oleosomes content. Structural factors in polymer chain conformation play an essential role in bridging flocculation efficiency. This study, as mentioned above, showed that polysaccharide surface charge is not the only factor influencing bridging flocculation but also polymer chain flexibility. Despite presenting a negative charge, xanthan gum could not induce bridging flocculation of soybean oleosomes, while alginate effectively induced bridging flocculation. This was attributed to the relative flexibility of alginate polymer chains instead of xanthan gum, which is modeled as a stiff, rod-like structure.

The present study investigated the bridging mechanism of another anionic polysaccharide with flexible polymer chains, such as *l*-carrageenan. It belongs to the carrageenan family (κ , ι , and λ), and it is a high molecular weight polysaccharide formed by galactose units and 3, 6-anhydrous-D-galactopyranosyl ring joined together by alternating glycosidic linkages. A previous study (Wu *et al.*, 2011) found that *l*-carrageenan was more effective at creating charged interfaces in soybean oleosomes than κ - and λ -carrageenan. This was attributed to the densely charged helical structure of *l*-carrageenan favoring electrostatic interactions with oleosomes interface. It may thus be worthwhile to probe the bridging ability of *l*-carrageenan on soybean oleosomes and compare it with another anionic polysaccharide that proved effective in bridging flocculation, i.e., alginate. Both polysaccharides are similar in which they present similar molecular weight, are negatively charged, and present relatively flexible polymer chains. However, they differ in how their structural backbone is arranged, having *l*-carrageenan as a repeating galactose unit, while alginate is arranged in a random sequence of blocks of D-mannuronic acid (M) and L-guluronic (G).

Therefore, the focus of the present study is to compare the effect of two anionic polysaccharides with flexible chains on the bridging capacity of soybean oleosomes. In order to induce polymer bridging flocculation, electrostatic attractive interactions are triggered by gradually lowering the pH to values where both polysaccharide and oleosome become oppositely charged. The interactions between alginate, *l*-carrageenan, and oleosomes over a range of pH values (3.00–8.00) are compared, followed by analyzing the effect of polymer/oleosome ratio and oleosome content on the rate of network contraction, particle size, and flocculation efficiency. Finally, confocal laser scanning microscopy (CLSM) will be used and compared to percolation gelation models. These considerations provide a consistent correlation between rheological properties and microstructures of the oleogels.

II. MATERIALS AND METHODS

A. Materials

Commercially available soybeans were acquired from Rapunzel Naturkost GmbH (Legau, Germany) and were used to extract oleosomes. TIC Gums, Inc. (Belcamp, MD) supplied sodium alginate

(TICA-algin 400 Powder) for the experiments. Carl Roth (Karlsruhe, Germany) provided iota carrageenan. All solutions were prepared using distilled water.

B. Sample preparation

Extraction of soybean oleosomes is based on an aqueous extraction method (Waschatko *et al.*, 2012) that yields oleosome cream free of soybean storage proteins (i.e., glycinin, β -conglycinin, Gly m BD 30 K). Soybeans are ground (Vorwerk Thermomix TM31) in a 1:10 soybeans/water ratio at 102 000 rpm for 90 s. The resulting slurry was filtered through two layers of Kimtech wipes 21×11 cm (Kimberly Clark), and soybean milk was obtained. Following filtration, the pH of the milk was brought down to 11.0 with 1 N NaOH (VWR Chemicals), and 25 wt. % sucrose was added. 50-ml Roth centrifuge tubes were used to fill the solution, which was centrifuged at 15 000 xg at 4 °C for at least 5 h. The resulting oleosomes were present as an upper cream layer collected with a spoon and then re-dispersed in a 20 wt. % sucrose solution with pH adjustment (11.0). Two more washing and centrifugation steps (15 000 xg, 4 °C, 5 h) were completed. The oleosome content of the resulting cream was determined by a halogen dryer and ranged between 50 and 60 wt. %. The concentrated cream was used as stock to dilute emulsions. The theoretical values of the three major components of soybean oleosome were estimated according to a model developed by Huang, 1992. The model calculates theoretical values of oleosome components according to the oleosome diameter size. Soybean oleosomes obtained from this protocol resulted in a 0.350 μm diameter size. As a result, the estimated amounts are as follows: 3.3% (w/w) phospholipids, 5.2% (w/w) protein, and 91.5% (w/w) triglycerides.

Oleosome emulsions were diluted with distilled water to create different concentrations (w/w), depending on the nature of the experiments. Starting from pH 7.0, dried sodium alginate and ι -carrageenan samples were added to the oleosome dispersions at different concentrations while keeping the same mass ratios (g polysaccharide/g oleosome). Polysaccharides/oleosome mixtures were stirred for a minimum of 20 h at 25 °C to guarantee proper hydration. Next, the pH of the mixtures was gradually lowered to 4.0 via dropwise titration with HCl at 1.0, 0.5, 0.1, and 0.01 N at a constant stirring speed (450 rpm) at 25 °C. Following pH adjustment, samples were either used immediately for further experiments or were centrifuged (5000 xg, 4 °C, 20 min) for experiments described in Sec. II G.

C. Demixing experiments

5 wt. % oleosome emulsions of alginate and carrageenan (0–0.125 wt. %) were left in sealed glass tubes at 25 °C to follow the demixing dynamics. Demixing was monitored over 18 days by visually following the cream's height as it separates from the supernatant. Initial height, H_0 , of emulsion samples was 10 ± 0.8 cm. Change in cream height became more significant in the first 2 h after preparation. As a result, data points became less frequent after the first day. The height of the collapsing network at time t was defined as $h(t) = H(t)/H_0$. The rate at which the network contract ν was obtained from the demixing curves and established where the cream contraction was more significant (120 min). It was determined by $\Delta H(t)/\Delta t$.

D. Particle size measurements

Oleosome–polysaccharide mixtures were diluted from 5 wt. % to approximately 0.5 wt. % (that is, 1:10) using buffer solution (same pH 4.00 as the sample being analyzed) to avoid multiple scattering effects. The particle size distribution of the emulsions was determined using a laser diffraction particle analyzer (LS 13320 Beckmann Coulter, CA). Measurements were performed using a laser diode with $\lambda = 780$ nm and three polarization intensity differential scanning (PIDS) wavelengths at $\lambda = 450, 600,$ and 900 nm. The data were analyzed using the instrument software applying Mie theory and using refracting indexes as follows: soybean oil and water 1.47 and 1.33, respectively. Four to five emulsion droplets were placed into the sampler chamber and then recirculated through the optical measurement cell. The mean particle size was reported as the volume-weighted value, d_{43} . Results were reported as the average of three measurements.

E. ζ -potential measurements

Oleosome emulsions of 0.2 wt. % were created by diluting concentrated cream stock, and the same procedure in Sec. II B was repeated (polysaccharide addition, pH adjustment to 4.0) while maintaining the same ratios from the other experiments. Diluted emulsions were injected directly into the measurement chamber of a particle electrophoresis instrument (Malvern Zetasizer Nano Z) that measures the direction and velocity of droplet movement in the applied electric field. An individual ζ -potential measurement was determined from the average of three readings taken on the same sample.

F. Microscopic imaging

5 wt. % polysaccharide–oleosome mixtures from Sec. II D. were observed in parallel by optical microscopy using a Carl Zeiss Axio Scope.A1 microscope (Carl Zeiss AG, Oberkochen, Germany). Images were captured by using transmission bright-field microscopy with the objective lenses magnifying $10\times$. ImageJ software was used to insert the scale bar. A drop of the emulsion was placed on a microscope slide and then covered with a coverslip. Confocal laser scanning microscopy (CLSM) was used to analyze the microstructure of bridging flocculated emulsion for 20 wt. % oleosome. CLSM was performed using a Zeiss Axiovert 200M (Oberkochen, Germany). Nile Red at 1 mg/ml, a fluorescent label excited at 543 nm with a helium–neon laser, was added in a 1:2000 ratio to stain the oil core of the oleosome droplets. 500 μL of the different mixtures was placed inside eight well-chambered borosilicate coverglass systems (Nunc Lab-Tek, Thermo Fisher Scientific). The obtained CLSM images were analyzed using the “ImageJ” software package.

G. Bridging efficacy of polysaccharides

Polymer-bridged gels, upon densification, were collected and quantified to analyze the bridging efficacy of alginate and carrageenan. After centrifugation, the transparent supernatant was decanted, and the compacted cream gels were collected and immediately weighed for the determination of the concentration in the gel. The concentration in the cream (oleosomes), C_g , is then given by

$$C_g = \frac{X_1}{X_2} C_e, \quad (1)$$

where C_e is the initial concentration of oleosomes before centrifugation, X_1 is the amount in grams of the initial oleosome dispersion, and X_2 is the amount in gram of the concentrated oleosome cream after centrifugation.

H. Rheological measurements

In order to investigate their resulting viscoelastic properties, oscillatory rheology was performed on the bridged-flocculated emulsions from 10 to 40 wt. % oleosome. Measurements were performed with a Bohlin Instruments Gemini 200 rheometer (Malvern Panalytical Ltd., Malvern, UK) equipped with a 25-mm parallel plate geometry. The gap size was adjusted stepwise to the thickness of the gels until the load in the force was detected, leading to gap sizes between 1000 and 1500 μm . After loading, a 5-min waiting period at 25 °C was used to allow the structure of the sample to relax before the measuring process began. Oscillatory amplitude sweeps were performed by increasing the strain logarithmically from 0.01% to 1000% at 1 Hz. All measurements were performed in triplicate at 25 °C from different batches, and all samples were prepared individually.

I. Characterization of polysaccharides

The molecular conformation of sodium alginate and iota carrageenan was determined by gel permeation chromatography combined with multi-angle light scattering (GPC-MALLS). Polysaccharides were dissolved in 0.1 M LiNO_3 . Measurements yielded distributions of molecular mass, M_w and radius of gyration, R_g . The measurements also provide ζ -potential values at pH 7.0 by dissolving both polysaccharides in phosphate buffer. Averages are given in Table I.

J. Theoretical models describing gelation

Particle gel systems usually show a power-law scaling behavior between the storage modulus G' and the concentration, c , of dispersed particles (Mellema *et al.*, 2002). Therefore, they can be described using different gelation models to give information on the type of deformation within the emulsion droplet network originating from the type of droplet-droplet interaction (Mellema *et al.*, 2002; Roulet *et al.*, 2021; and Xi *et al.*, 2019). Percolation theory is known for its general applicability in particle gel systems, e.g., colloidal particles, protein gel systems, and bridging-flocculated systems (Blijdenstein *et al.*, 2004b; Diedericks *et al.*, 2019; van der Linden and Sagis, 2001; Veerman *et al.*, 2003; and Veerman *et al.*, 2002). The percolation model shows a critical percolation threshold, c_p , which has been shown to be dependent on the polysaccharide type (e.g., charge distribution) and also to parameters that affect molecular interactions, e.g., pH and ionic strength (van der Linden and Sagis, 2001).

TABLE I. Molecular characterization of alginate and carrageenan. M_w is the weight-averaged molecular weight, surface charge expressed by zeta potential measurements at pH 7, and R_g is the radius of gyration.

Polysaccharide	M_w (g/mol)	Surface charge (mV)	R_g (nm)
Sodium alginate	250 000	-55.19 ± 8.29	62
Iota carrageenan	300 000	-28.36 ± 10.49	63

For random percolating systems, the elastic shear modulus shows a scaling law as shown in the following equation:

$$G' \propto (c - c_p)^t, \quad (2)$$

where c is the oleosome concentration, c_p is the critical percolation threshold concentration, and t an exponent. The exponent t depends on the type of forces between network elements that leads to the elastic rigidity of an irregular (particle) network where it can range from central stretching forces to bond-bending forces (Blijdenstein *et al.*, 2004b).

III. RESULTS AND DISCUSSION

A. Flocculation characterization of polysaccharide-oleosome mixtures.

1. Demixing behavior and microstructural properties

Curves of the process of network contraction are shown in Fig. 1. In the absence of polysaccharides, the oleosome dispersion remains stable until 10⁴ min, when the cream collapses. As suggested in Zambrano and Vilgis (2023), this type of demixing indicates the gradual increase in the size of the flocs, which causes sufficiently large flocs to cream faster as a result of density difference according to the Stokes law (Chang and Liao, 2016). At 0.0025 wt. %, alginate and carrageenan-containing mixtures present similar rates of network contraction, but network contracts to a greater extent in alginate-containing mixtures [Fig. 1(a)]. Figure 1(c) shows the presence of oil on top of the cream network indicating signs of droplet coalescence. Carrageenan-containing mixtures presented no signs of droplet coalescence, suggesting that a more stable droplet network is formed. Both carrageenan and alginate oleosome-containing mixtures present instant flocculation at 0.025 wt. % shortly after pH adjustment to 4.0. This is reflected in the short time frames at which the network contracts in the first minutes after preparation [Figs. 1(a) and 1(b)]. Optical microscopy images also show large and heterogeneous aggregates for both polysaccharides at 0.025 wt. % [Figs. 3(b) and 3(g)]. Intensive aggregation at 0.025 wt. % alginate indicates polymer bridging, which corresponds to a mass ratio of 0.005 g/g (g polysaccharide/g oleosome). As observed previously (Zambrano and Vilgis, 2023), 0.005 g/g corresponds to the ratio where optimum bridging occurs for alginate. Carrageenan induces a similar bridging mechanism, while the maximum bridging ratio also seems to be around 0.005 g/g. However, when comparing network contraction rates (ν) [Fig. 2(c)], carrageenan showed lower ν , 10.20 mm/h, than alginate, 18.33 mm/h indicating a seemingly less intense aggregation in carrageenan. This observation is also reflected in Fig. 2, which shows a closer look at the gel heights over time at the two ratios that present intense aggregation, 0.005, and 0.01 g/g. It can be observed that the network compresses to a lesser extent in carrageenan-containing mixtures for both ratios, being more evident at 0.005 g/g, where there is a significant difference in network height between alginate- and carrageenan-containing mixtures. At 0.01 g/g oleosome, on the other hand, ν is higher in carrageenan-containing mixtures (4.80 mm/h) than in alginate-containing mixtures (1.91 mm/h), indicating a greater extent of aggregation. This agrees with microscopy images where larger aggregates are observed for carrageenan-containing mixtures compared to alginate at 0.05 wt. % (0.01 g/g) [Figs. 3(c) and 3(h)]. Aggregates in alginate-containing mixtures instead start to be less dominant at >0.05 wt. % [Figs. 3(d) and

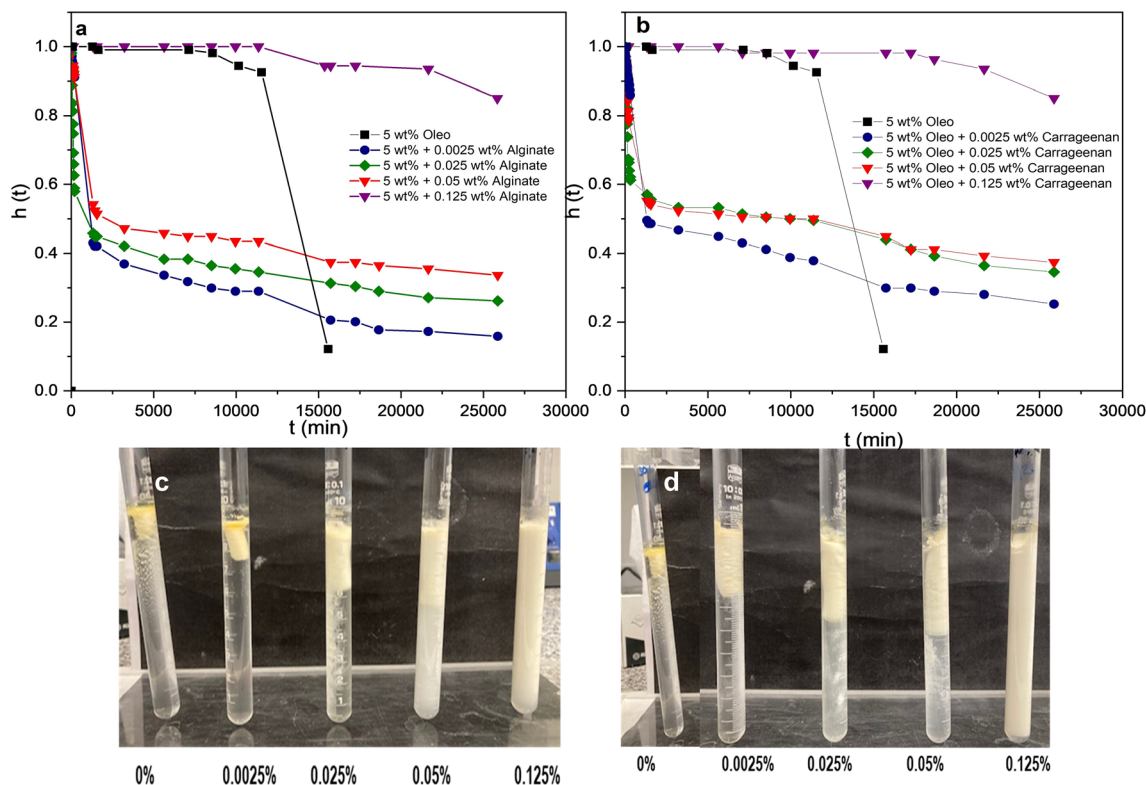


FIG. 1. Demixing experiments of 5 wt. % oleosome with different polysaccharide concentrations after being adjusted to pH 4.00. (a) Plot of network height, $h(t)$, vs time of alginate-containing mixtures, (b) plot of network height, $h(t)$, vs time of carrageenan-containing mixtures, (c) visual appearance of alginate-containing mixtures after 150 min, (d) visual appearance of carrageenan-containing mixtures after 150 min.

3(e)]. Figure 1(c) shows 0.05 wt. % alginate presenting a turbid supernatant, indicating that alginate polymer chains stabilize some oleosome droplets. In contrast, 0.05 wt. % carrageenan presents a transparent supernatant, suggesting that at this ratio, all oleosome droplets are still effectively bridged by the carrageenan polymer chains. This indicates that polymer bridging in alginate becomes less effective at 0.01 g/g, and carrageenan can still bridge oleosome droplets at 0.01 g/g. On the contrary, carrageenan seems more effective at stabilizing oleosome droplets as observed in Fig. 3(i), where at 0.125 wt. %, aggregates completely disappear. In comparison, alginate still shows the presence of separate clusters at 0.125 wt. % [Fig. 3(d)]. This is also observed in particle size distribution where the peak around $0.350 \mu\text{m}$, indicating intact oleosome droplets, becomes more predominant in carrageenan at earlier concentrations than in alginate 0.125 and 0.175 wt. % [Figs. 3(e), 3(d), 3(i), and 3(h)]. This indicates that carrageenan is more effective at fully covering the oleosome surface at lower concentrations than alginate, despite presenting a decreased bridging ability compared to alginate. These results can be attributed to the different physical properties of the alginate and carrageenan chains.

2. Polymer physics analysis

The structural differences between alginate and carrageenan chains require some attention. Alginate is a block polyelectrolyte composed of charged guluronic and polar mannuronic acids, whereas carrageenans

are uniformly charged along their chains. The charged blocks in alginate, shown as blue zig-zag lines in Fig. 4, can be seen as relatively stiff due to chemical structure and bonds of the guluronic acid. The mannuronic and mixed (polar) blocks (shown as gray lines) are very flexible.

For the sake of simplicity, the conformation of carrageenan is described by simple models for polyelectrolytes, as suggested some time ago by De Gennes (1979). Not every monomer can release its counterion, which means that the chain pieces between the charges are coiled for entropic reasons. The balance between the electrostatic repulsive forces and the entropy loss by stretching yields the blob model suggested in Fig. 4. The chains are stretched on large scales, whereas inside the blobs the chains are coiled. The electrostatic blob size ξ_e depends on the charge fraction f and the Bjerrum length l_B . Simple scaling estimates suggest, for example, $\xi_e \cong \left(\frac{l_B f^2}{b}\right)^{-1/3}$, where b is the effective monomer size. The “chain of blobs” is consequently stretched, as shown in Fig. 4.

The primary mechanism of the adsorption of the different polysaccharides, as shown in Fig. 5, depends on their architecture and physical properties. Due to electrostatic interactions, the negatively charged alginate blocks adsorb strongly on the positively charged oleosome surfaces. The polar (uncharged) blocks, which separate the charged blocks allow for many degrees of freedom. The overall flexibility of alginate is thus high. According to Table I, the mean molecular weight of carrageenan is about 300,000 g/mol, which yields about 300

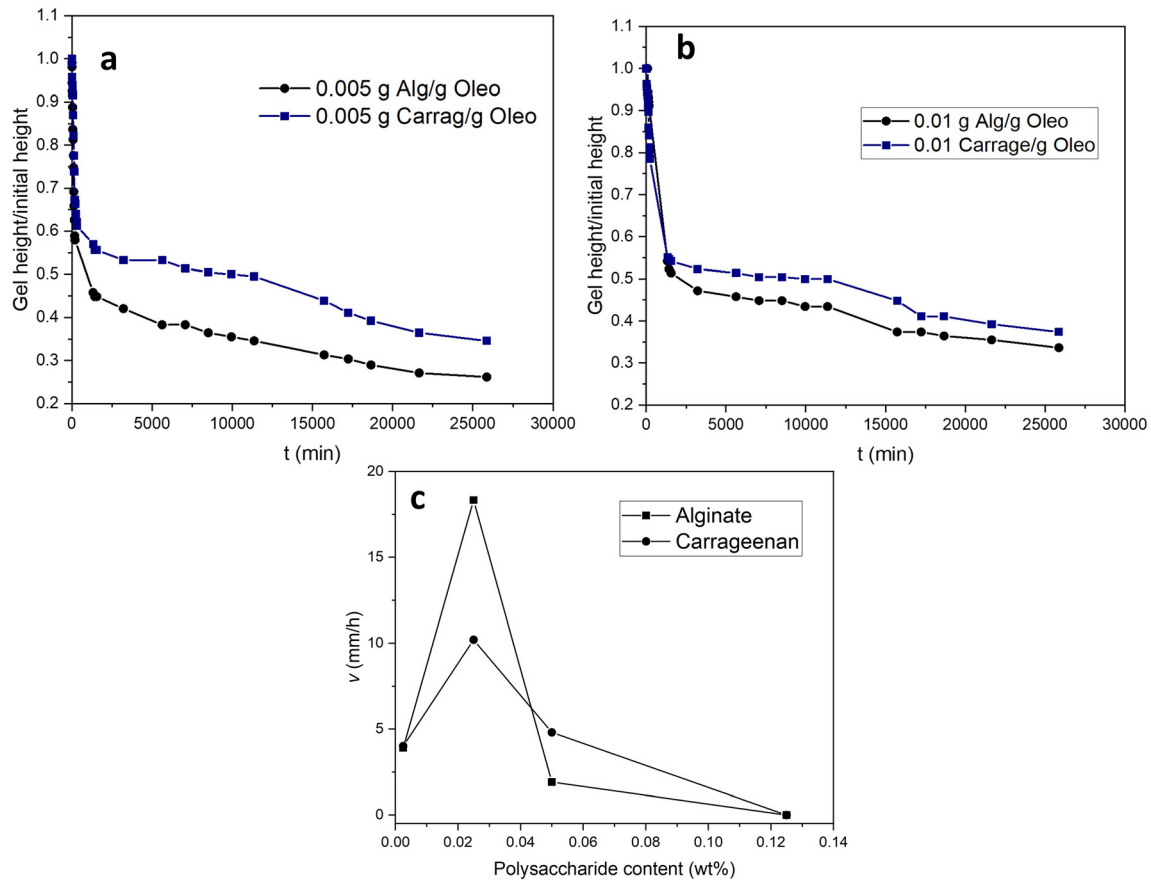


FIG. 2. Comparison of network height vs time at two ratios of alginate and carrageenan. (a) 0.005 g polysaccharide/g oleosome, (b) 0.01 g polysaccharide/g oleosome, and (c) network contraction rates (v) extracted from Figs. 1(a) and 1(b).

monomer units, which implies chains around 20 electrostatic blobs in a very rough estimate, by assuming the Bjerrum length of about 0.7 and 0.9 μm (in water). The values shown in Table I suggest the blobs have a size of about 5 nm (assuming the Kuhn length is about ten monomers). Of course, these estimates are very crude, but the results allow us to understand the observer experimental differences between alginate and carrageenan more consistently.

Carrageenan is represented as a chain of blobs but is less flexible on a larger scale, $r > \xi$. By bending according to the oleosome surface, it adsorbs strongly. As a result, it neutralizes parts of the oleosome charge, as illustrated in Fig. 5. Therefore, oleosomes can be easily coated in monolayers at appropriate carrageenan concentrations but are bridged less effectively by carrageenan, especially when the chains are not sufficiently long. This naïve idea suggests a weaker tendency to form strong flocculated clusters, in contrast to alginate chains. Another consequence of the different basic structures is worth mentioning, which becomes important for the mechanical and rheological properties of solutions and gels containing these polymers and oleosomes. Because of the strong electrostatic repulsion, carrageenan chains will (at normal concentrations and without added monovalent salts) not be able to entangle at concentrations larger than the overlap concentration c^* (Dobrynin and Jacobs, 2021; Matsumoto et al., 2021).

On the contrary, alginate chains can especially within the neutral blocks (Ahn et al., 2019; Nie et al., 2008). The viscoelastic properties of the solution will be different already at this simple level, as illustrated in Fig. 6.

Entanglements are topological restrictions. Thus, they act at specific time scales and deformations as temporary crosslinks (Doi and Edwards, 1988). These points will become important, as it is demonstrated in Secs. III B–III F.

B. Bridging flocculation characterization

Figures 7(a) and 7(b) shows the summary of mean particle sizes, d_{43} , as a function of polysaccharide/oleosome mass ratios at three different oleosome concentrations. The plots show prominent peaks in d_{43} , reflecting the ratio at which optimum bridging occurs, followed by a drop at higher polysaccharide/oleosome ratios indicating droplet re-stabilization. It can be observed that, in general, alginate-containing mixtures showed larger d_{43} values than carrageenan-containing mixtures. On the other hand, alginate-containing mixtures present three sharp peaks centered at 0.005 g/g, while the largest d_{43} in carrageenan-containing mixtures does not show a single peak centered at one specific ratio; instead, it is expanded between 0.005 and 0.01 g/g. This

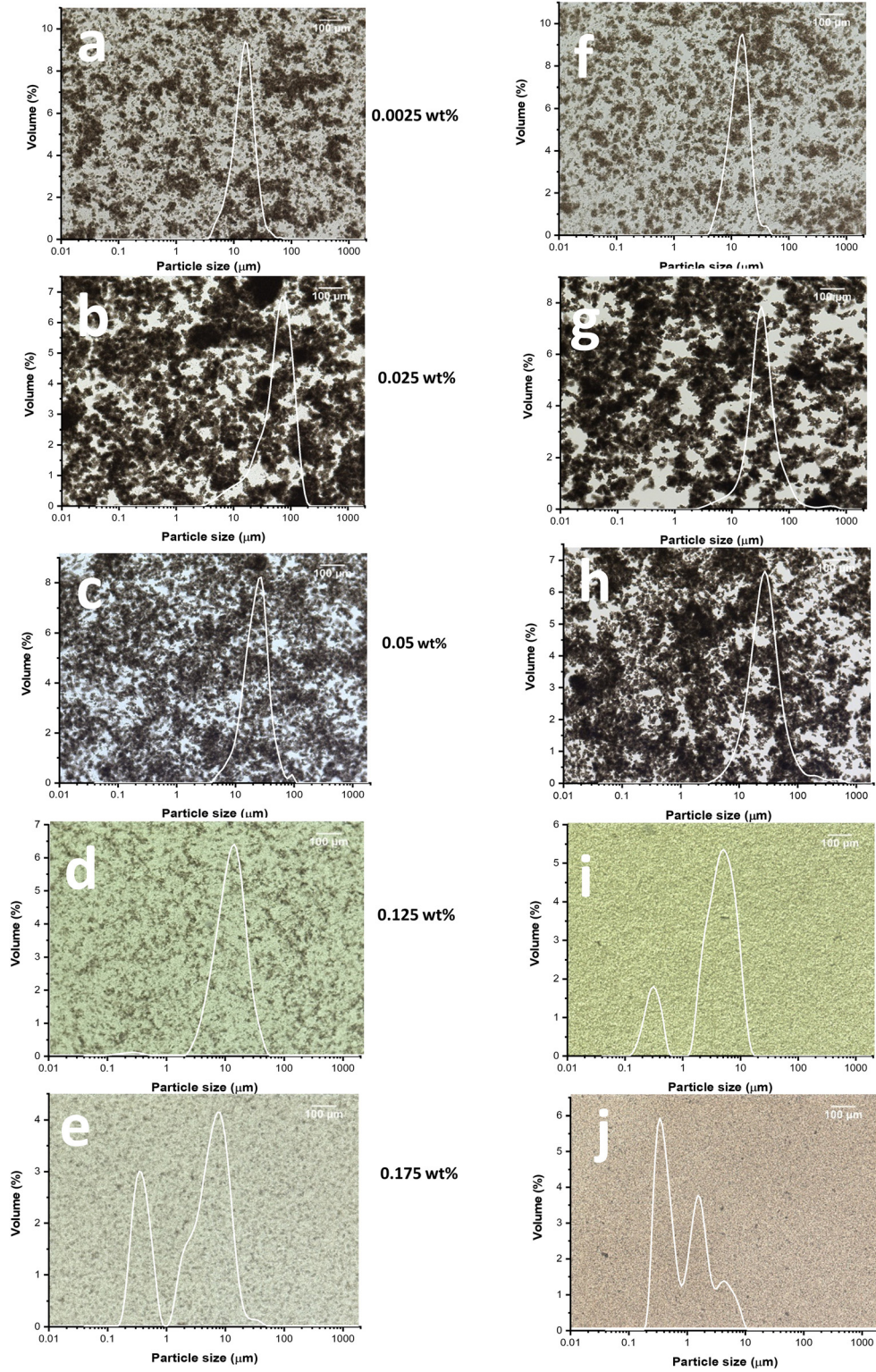


FIG. 3. Optical microscopy images of oleosome 5 wt. % at different polysaccharide concentrations after being adjusted to pH 4.0 combined with particle size distributions. In (a)–(e), emulsions contained different concentrations of alginate. In (f)–(j), emulsions contained different concentrations of *ι*-carrageenan. Scale bar: 100 μm .

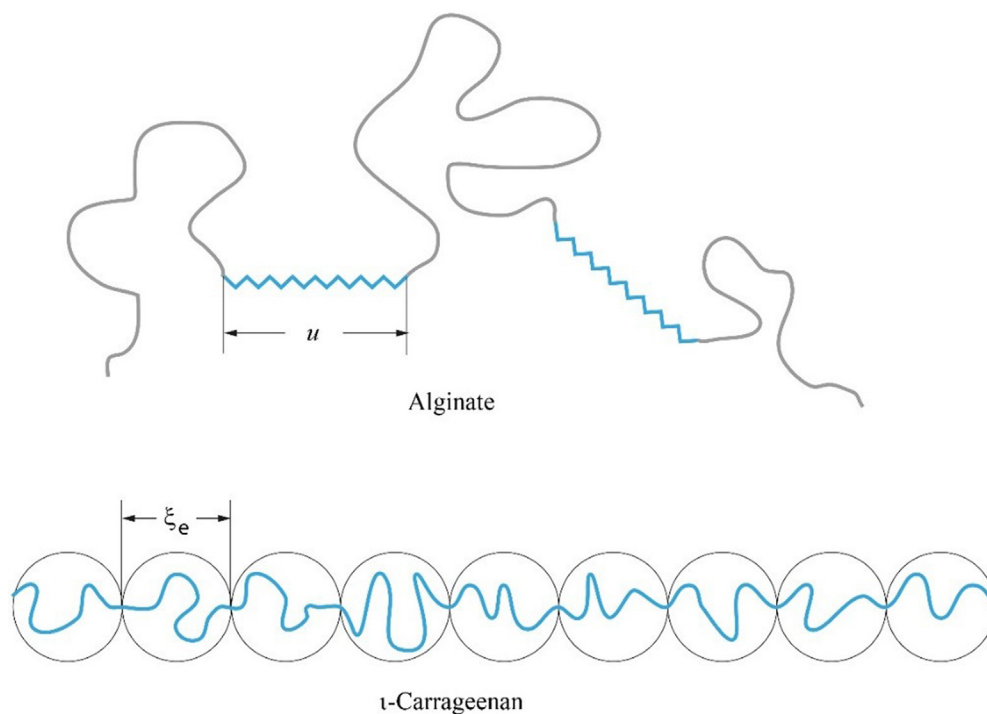


FIG. 4. Simple models of the physical properties of alginate and carrageenan. In alginate, only the guluronic blocks (shown in blue) can be charged, and the polar blocks behave as flexible chains in good solvents. Carrageenans are weakly charged polyelectrolytes in good solvents, illustrated in a simple blob model based on scaling ideas (De Gennes, 1979).

greater width of the flocculation peak in carrageenan indicates a weaker binding affinity of the carrageenan polymer chains with the oleosome interface. In previous studies (Dickinson and Pawlowsky, 1998; Lips *et al.*, 1991), it was also found that a broader flocculation peak by bridging polymers indicates weaker interfacial interaction between polysaccharide and droplet surface. These observations are

aligned with previous demixing plots and indicate that carrageenan may produce less intense bridging than alginate. These issues are analyzed further in Fig. 7(c), where the polysaccharide concentration plotted at which maximum aggregation occurred at the different oleosome concentrations. It can clearly be observed that alginate produces a perfect linear regression fit ($R^2 = 1.0$), while carrageenan presents a lower value ($R^2 = 0.84$). The relatively low value for carrageenan, however, is largely due to the limited amount of polysaccharide/oleosome ratios studied, rather than a true discrepancy. The slopes of the linear fitting result in 0.005 and 0.01 for alginate and carrageenan, respectively, agreeing with the polysaccharide/oleosome ratios discussed above. The difference in optimum ratios for bridging flocculation confirms that carrageenan is less efficient than alginate for polymer bridging, as more carrageenan polymer chains are needed to flocculate the same amount of oleosome droplets. These ratios correspond to an interfacial coverage of approximately 0.4 and 0.8 mg/m^2 for alginate and carrageenan, respectively. These values for carrageenan are in agreement with other findings for bridging-flocculated emulsions (Dickinson and Pawlowsky, 1998), while for alginate, the value is closer to bridging-flocculated emulsions induced by highly charged polysaccharides such as dextran (Dickinson and Pawlowsky, 1996).

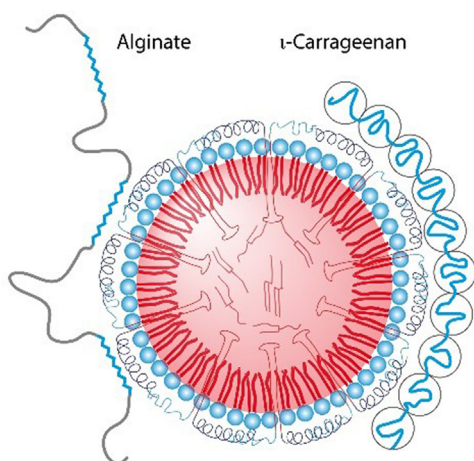


FIG. 5. Alginate and ι -carrageenan adsorb differently on the oleosome surface (drawn not to scale). Carrageenan gains most energy, when the chain of blobs bends according to the oleosome surface, without losing much entropy.

1. Bridging flocculation efficiency of polysaccharides

A simple bridging efficiency test was performed to confirm whether carrageenan or alginate is more efficient for bridging. As bridging flocculation effectively separates the cream from the supernatant, the concentration after centrifugation is a good measure of how

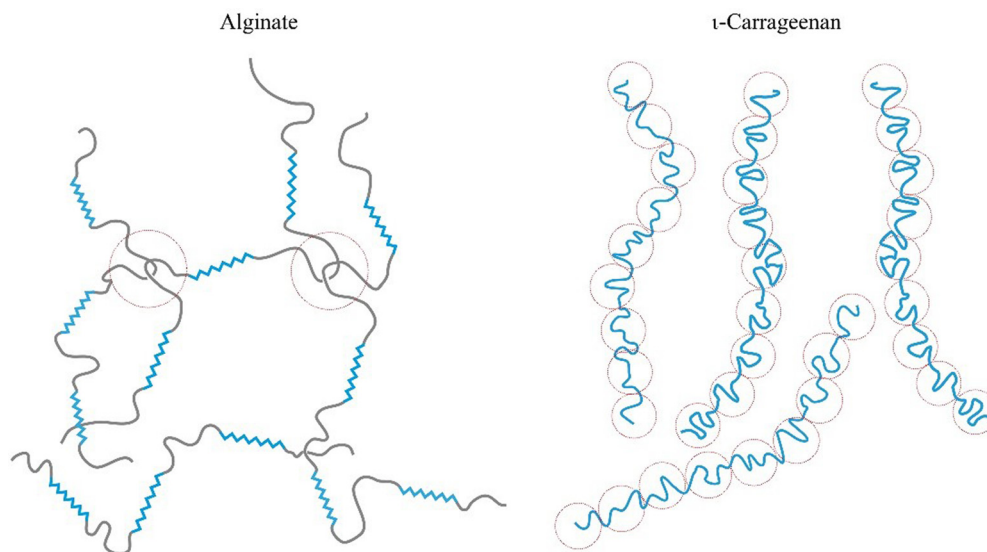


FIG. 6. Conformation of chains in alginate and ι -carrageenan solutions. Alginate chains are assumed to be able to form entanglements (red circles) at the polar, flexible blocks in concentrated (calcium free) solutions. The negative charges (visualized by the electrostatic blob diameter) prevent the formation of entanglements in carrageenan. The closer the blobs come, the stronger is the Coulomb repulsion between the charges.

effectively a polysaccharide can bridge oleosome droplets. Bridging-flocculated emulsions at different initial oleosome contents were centrifuged and quantified according to Eq. (1). To this end, the higher the cream content (oleosomes wt. %) after centrifugation, the more effective bridging is (Fig. 8). Here, the optimum bridging ratio between alginate and carrageenan ratios is compared.

At all oleosome contents, 0.005 g/g alginate yields the most concentrated gels. For example, starting at 40 wt. % oleosome, alginate can yield gels of roughly 64 wt. %, whereas carrageenan yields up to 57 wt. %. Alginate-containing mixtures can be compacted to yield approximately 45 wt. % starting at 5 wt. % oleosome, while carrageenan produces about 42 wt. % starting at 5 wt. % oleosome. While this difference in bridging efficiency is more significant at the ratio alginate presents optimum bridging (0.005 g/g), it is less clear at 0.01 g/g as alginate becomes less efficient for bridging. The individual oleosomes are already coated, and the space for interconnecting chains is very much restricted. Carrageenan, at 0.01 g/g, yields more compact gels only at 20 and 40 wt. % oleosome resulting in 49 and 60 wt. %, respectively. Overall, alginate is more efficient in yielding more concentrated gels than carrageenan. This is expected since, as previously described, carrageenan adsorbs weaker than alginate on oleosome surfaces.

C. Effect of pH on polysaccharide adsorption

To better understand the nature of the interactions between alginate, carrageenan, and oleosomes, ζ -potential measurements were performed. The addition of alginate and carrageenan to the oleosome droplets caused an appreciable change in the oleosome net charge depending on the pH and polysaccharide concentration [Fig. 9(a)]. The change in ζ -potential was calculated [Fig. 9(b)] at each pH: $\Delta\zeta = \zeta_2 - \zeta_1$, where ζ_2 and ζ_1 are the ζ -potentials of the polysaccharide-oleosome mixture and bare oleosome droplet, respectively. At pH

> 6.00, the decrease in oleosome net charge is not significant as both polysaccharide and oleosome present negative charges and chances of electrostatic interactions are minor. However, it can be observed [Fig. 9(b)] that alginate decreased oleosome charge slightly more than carrageenan. Electrostatic interactions occurring at neutral pH are characteristic of highly charged polysaccharides where the polymer chains adsorb on a few positive charged patches on the oleosome-charged interface (Dickinson and Pawlowsky, 1996). At pH 4.00, the change in oleosome charge density was appreciably more significant for both polysaccharides, which caused charge reversal of oleosome net charge from positive to negative charge density, especially for polysaccharides concentration >0.0001 wt. %. This indicates that electrostatic interactions strongly occur between polysaccharides and oleosome at the acidic range where both polysaccharides are oppositely charged. Nevertheless, alginate had the most significant overall change in oleosome net charge, as quantitatively shown in Fig. 9(b). A significantly greater change in charge in alginate supports the idea of a considerably stronger electrostatic interaction between alginate and oleosomes when compared to carrageenan. This is consistent with the surface charge of the pure polysaccharide solutions, as alginate presented a higher charge density than the carrageenan solution (Table I). Consequently, carrageenan can be considered a weakly charged polyelectrolyte (Dobrynin *et al.*, 1995). However, it is essential to consider that zeta potential values are relative values that consider the electrokinetic potential at the slipping plane; therefore, it is not easy to conclude these values as the absolute surface charge of the molecules. These results show that electrostatic interactions and charge density are the driving factors that induce polymer bridging flocculation for both polysaccharides when combined with oppositely charged particles. In the presence of a pH decrease from 7.00 to 4.00, both polysaccharides interact with the oleosome interface more strongly.

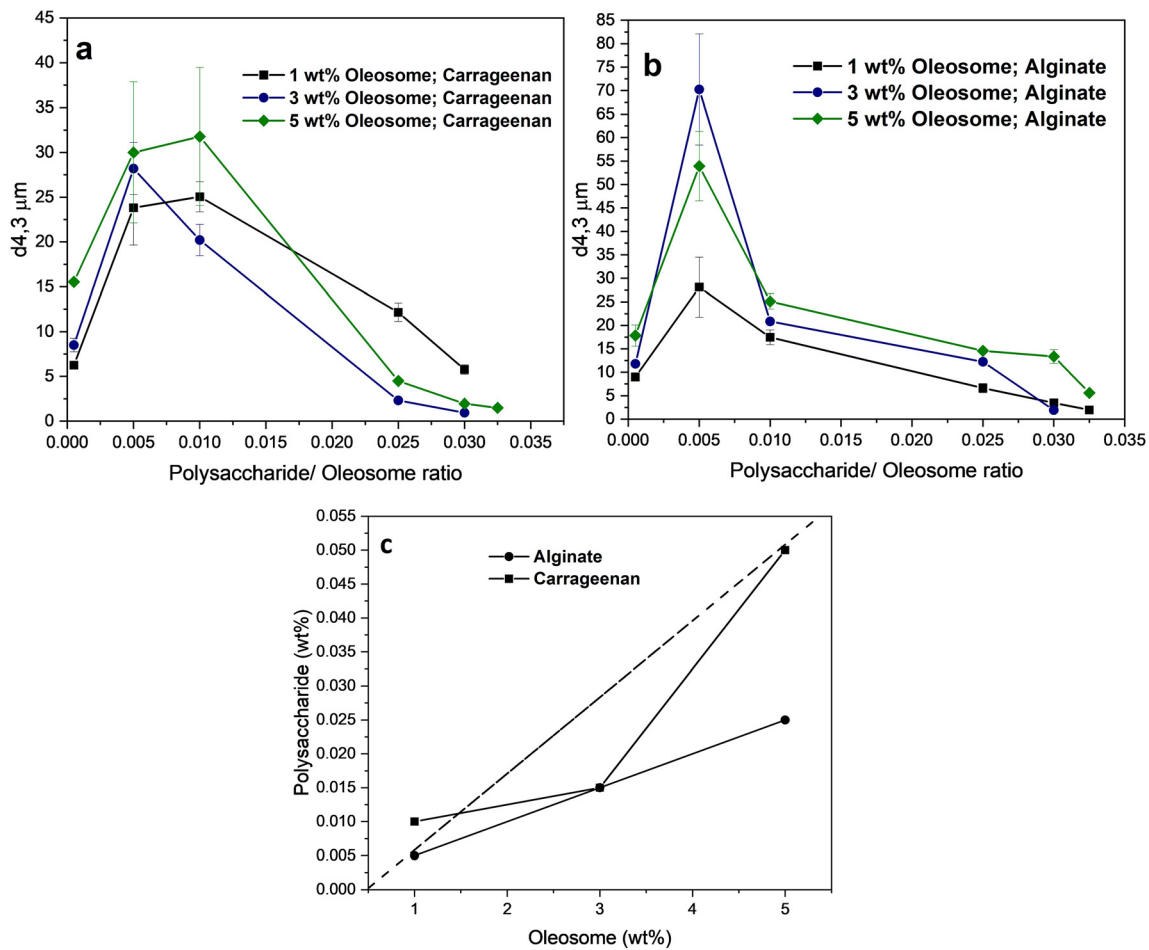


FIG. 7. Mean particle size ($d_{4,3}$) as a function of polysaccharide/oleosome ratios at three oleosome concentrations. (a) Carrageenan-containing mixture, (b) alginate-containing mixture, (c) plots of polysaccharide concentration (wt. %) vs oleosome content (wt. %) showing the concentration at which maximum bridging occurred.

D. Rheological characterization of bridging-flocculated emulsions at different oleosome contents

The results of the oscillatory strain sweeps of the mixtures at different oleosome content and fixed polysaccharide/oleosome ratios are summarized in Fig. 10. All the samples show $G' > G''$ at small strains ($\gamma < 20\%$), indicating solid-like character, and at larger strains ($\gamma > 20\%$) $G' < G''$, which indicates that the samples become a liquid-like material. The linear viscoelastic region (LVR) appeared to be independent of oleosome content presenting a critical strain (γ_0) of about 3% in all samples when considering the definition of a 10% deviation in G' from its maximum value. Overall, at $\gamma > 3\%$ G' decreases faster than G'' in all samples, which is associated with the fracture behavior of a particle gel-like structure (Zambrano and Vilgis, 2023). However, among the samples, G' and G'' will decrease either sharply or gradually depending on the polysaccharide type and the polysaccharide/oleosome ratio. To measure the steepness of the decrease in modulus, the slope was measured for the strain region between $\gamma = 3\%$ and 100% (Table II). The parts that follow will go into greater detail about these findings.

1. Percolation theory

In the LVR for all samples, G' ($\gamma = 0.5\%$, $\omega = 10 \text{ rad s}^{-1}$) increases with oleosome content in a power-law fashion, as shown in Fig. 11. By plotting G' against the oleosome concentration on a double logarithmic scale, it is tempting to apply a percolation model to fit the dependence of G' on oleosome concentration. The critical percolation concentration (c_p) and the scaling exponent (t) as defined in Eq. (2) were determined using a method described by van der Linden *et al.* (van der Linden and Sagis, 2001). This approach uses plots of $G'^{1/t}$ vs c to determine the exponent t [see Eq. (2)] by providing arbitrary values that yield the best linear fits. From our results, the best fits were obtained for scaling exponent t , which yielded regression coefficients R^2 above 0.97, and an average c_p was determined. By using calculated c_p values, the actual t values could be obtained from the plots G' vs $(c - c_p)^t$. As shown in Table III, c_p values were between 0.16% and 0.40%. These values are in agreement with those reported for protein gel systems ($c_p = 0.3\% \pm 0.2\%$) (Veerman *et al.*, 2002) and ($c_p = 0.45\% \pm 0.25\%$) (Diedericks *et al.*, 2019), which presented stronger protein-protein attractions within the gel network due to

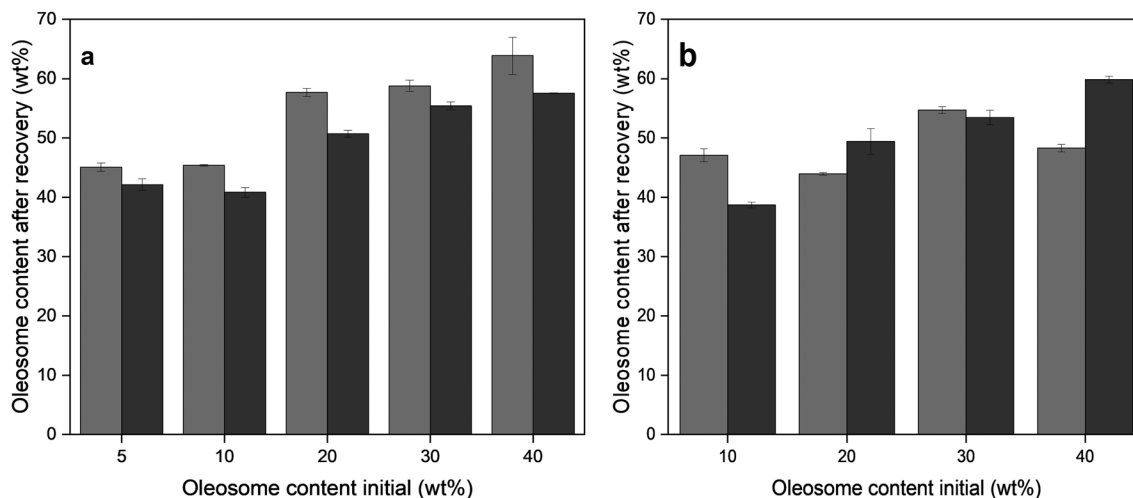


FIG. 8. Bridging performance of alginate (light gray bars) and carrageenan (dark gray bars) on oleosome droplets expressed as concentration of oleosomes after centrifugation recovery (wt. %) at: (a) 0.005 g polysaccharide/g oleosome and (b) 0.01 g polysaccharide/g oleosome.

increasing ionic strength values. In bridging-flocculated emulsions containing negatively charged carboxymethyl–cellulose (Blijdenstein *et al.*, 2004b), c_p was extrapolated to 0, attributed to the stronger bridging attraction between the oil droplets. Previous work from Segre *et al.* (2001) related c_p to the magnitude of the attractive interaction, U , between the emulsion droplets, where c_p decreased with increasing attractive energy. Therefore, our results further confirm that strong, attractive interactions drive flocculation in our systems. Furthermore, alginate presented the lowest c_p , 0.16%, confirming that the strongest bridging interaction occurred at 0.005 g/g alginate, but as bridging becomes less effective at 0.01 g/g, c_p increases to 0.39%.

The values for the scaling exponent t showed an average of 3.35, the highest at alginate 0.005 g/g ($t = 3.60$). The scaling exponent t is

somewhat higher than predictions from the isotropic percolation model ($t = 2.06 \pm 0.6$) (Kanai *et al.*, 1992), which was observed in diverse protein systems and describe their apparent homogeneous network architectures (van der Linden and Sagis, 2001). The higher t for our samples may indicate non-homogeneous network architectures, as similar values were reported for plant protein gels and pre-sheared systems, which are anticipated to be of this type (Diedericks *et al.*, 2019; Kanai *et al.*, 1992; and Trappe and Weitz, 2000).

E. Microstructural properties of flocculated emulsions

The microstructure of the bridging flocculated emulsions was examined using CLSM (Fig. 12). From the length scales of the CLSM

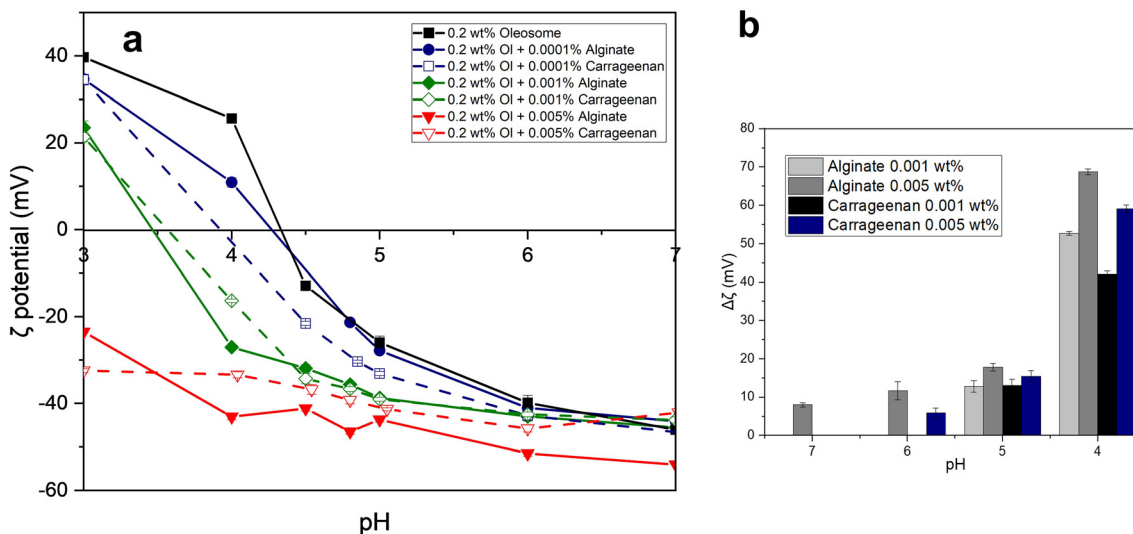


FIG. 9. (a) Zeta potential plots vs pH of 0.2 wt. % oleosome with different alginate and carrageenan concentrations and (b) the change in ζ ($\Delta\zeta$) between bare oleosome and polysaccharide-adsorbed oleosome at each pH was quantified and expressed as $\Delta\zeta$.

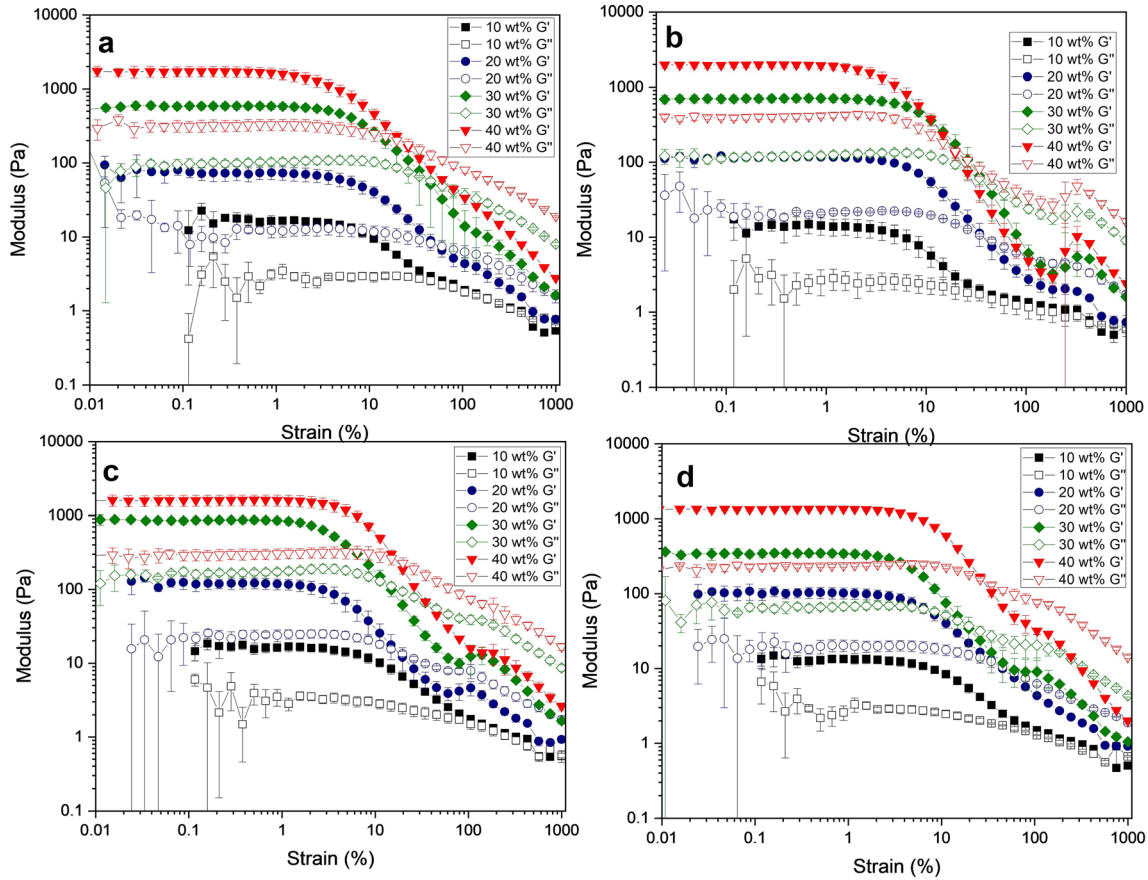


FIG. 10. Oscillatory rheology measurements of polysaccharide/oleosome mixtures at different oleosome contents and fixed at two polysaccharide/oleosome ratios. (a) 0.005 g carrageenan/g oleosome, (b) 0.005 g alginate/g oleosome, (c) 0.01 g carrageenan/g oleosome, (d) 0.01 g alginate/g oleosome.

images ($20\ \mu\text{m}$), the samples appear inhomogeneous to a different degree, where 0.005 g/g alginate at 5% and 20% oleosome presented the largest structures; therefore, inhomogeneous up to a much larger degree compared to the other samples. This is also consistent with its largest scaling exponent ($t = 3.60$) among the other samples obtained from the percolation model. In addition, the interpretation of the scaling exponent t leads to information on the forces between network elements that lead to elastic rigidity. In gel networks where bond-bending forces are also present, t values have resulted in 3.75 ± 0.11 (Sahimi

and Arbabi, 1993). These higher t values have been reported elsewhere where structures were characteristic of heterogeneous systems (Diedericks *et al.*, 2019; Grant and Russel, 1993; and Kanai *et al.*, 1992), and according to Kantor and Webman (Kantor and Webman, 1984), when $2.9 < t < 3.6$, both bond-bending and bond-stretching forces are present in the gel network. These forces correspond to the bending energy of the polymers because they define mainly the stiffness of the clusters, apart from steric and geometric restrictions, which define the deformation properties of the clusters. The exponent

TABLE II. Slope parameters obtained from oscillatory amplitude sweep measurements for strain values between 3% and 100%. $\gamma_1 = \sim 3\%$ and $\gamma_2 = \sim 100\%$ were chosen as the coordinates of first and second points for all samples. Note: Values are presented as the mean standard deviation \pm of at least duplicate values.

Oleosome	0.01 alginate		0.01 carrageenan		0.005 alginate		0.005 carrageenan	
	G'	G''	G'	G''	G'	G''	G'	G''
40%	-1.07 ± 0.02	-0.35 ± 0.00	-1.32 ± 0.07	-0.43 ± 0.02	-1.83 ± 0.02	-0.82 ± 0.02	-1.12 ± 0.07	-0.44 ± 0.03
30%	-0.98 ± 0.15	-0.35 ± -0.09	-1.05 ± 0.13	-0.40 ± 0.06	-1.49 ± 0.05	-0.56 ± 0.01	-1.10 ± 0.20	-0.33 ± 0.10
20%	-0.83 ± 0.04	-0.32 ± 0.03	-0.80 ± 0.07	-0.29 ± 0.06	-1.08 ± 0.06	-0.43 ± 0.02	-0.80 ± 0.04	-0.22 ± 0.01
10%	-0.66 ± 0.04	-0.25 ± 0.13	-0.64 ± 0.03	-0.25 ± 0.03	-0.61 ± 0.07	-0.22 ± 0.02	-0.58 ± 0.02	-0.08 ± 0.03

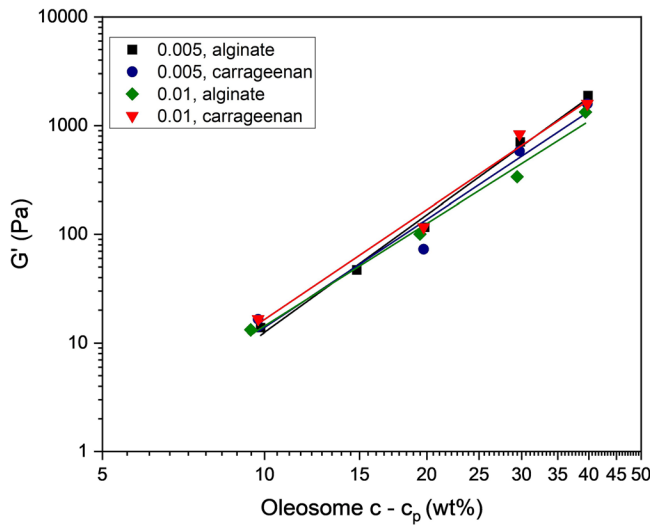


FIG. 11. Double logarithmic plot of G' (Pa) vs $(c - c_p)^t$.

suggests a mixed elastic behavior of the flocculated clusters. At local length scales, i.e., between two oleosomes, the different elastic stretching properties of the polymers play an essential role, whereas at larger scales, beyond the diameter of the oleosomes, steric hindrances between rigid oleosomes come into play.

Although percolation theory may be used to describe the network characteristics of the gels, the apparent structural heterogeneity of our samples coupled with the low c_p values may indicate that a fractal scaling model $G' \sim c^n$ (where c_p is zero) could be better suited (Mellema et al., 2002). The exponent n values observed in Table III are not significantly different from the exponent t values observed from percolation theory. This suggests that a fractal scaling approach could be

TABLE III. Scaling exponents n , t , and percolation threshold c_p for alginate and carrageenan containing bridging-flocculated emulsions at two mass ratios. Note: Values are presented as the mean standard deviation \pm of at least duplicate values.

	n	t	c_p
0.005 g/g, alginate	3.63 ± 0.15	3.60 ± 0.15	0.15 ± 0.76
0.005 g/g, carrageenan	3.35 ± 0.06	3.30 ± 0.06	0.24 ± 0.36
0.01 g/g, alginate	3.24 ± 0.11	3.17 ± 0.11	0.39 ± 0.44
0.01 g/g, carrageenan	3.41 ± 0.13	3.33 ± 0.12	0.40 ± 0.66

better suited to describe the gel network of bridging-flocculated emulsions.

Additionally, Fig. 12 shows the variation in microstructure between the different samples. In addition to the great degree of heterogeneity observed at 0.005 g/g alginate, the microstructure at 0.01 g/g alginate changes from a completely interconnected droplet network to a system formed by more homogeneous and separate clusters as the amount of alginate polymer chains over oleosome droplets increases, as previously observed in Figs. 3(d) and 3(e). This transition is caused by the alginate polymer chains that start to coat the oleosomes surface completely as discussed extensively in our previous publication. Carrageenan, however, displays more uniform and distinct clusters at 0.005 g/g, where its bridging effectiveness is lower, and on the other hand, 0.01 g/g carrageenan presents more interconnected and heterogeneous, confirming that optimum bridging in carrageenan occurs at a higher concentration than alginate.

F. Final discussion

To better understand the structural details, it appears helpful to summarize the results obtained in physical models based on Figs. 5 and 6 and now extended in Fig. 13.

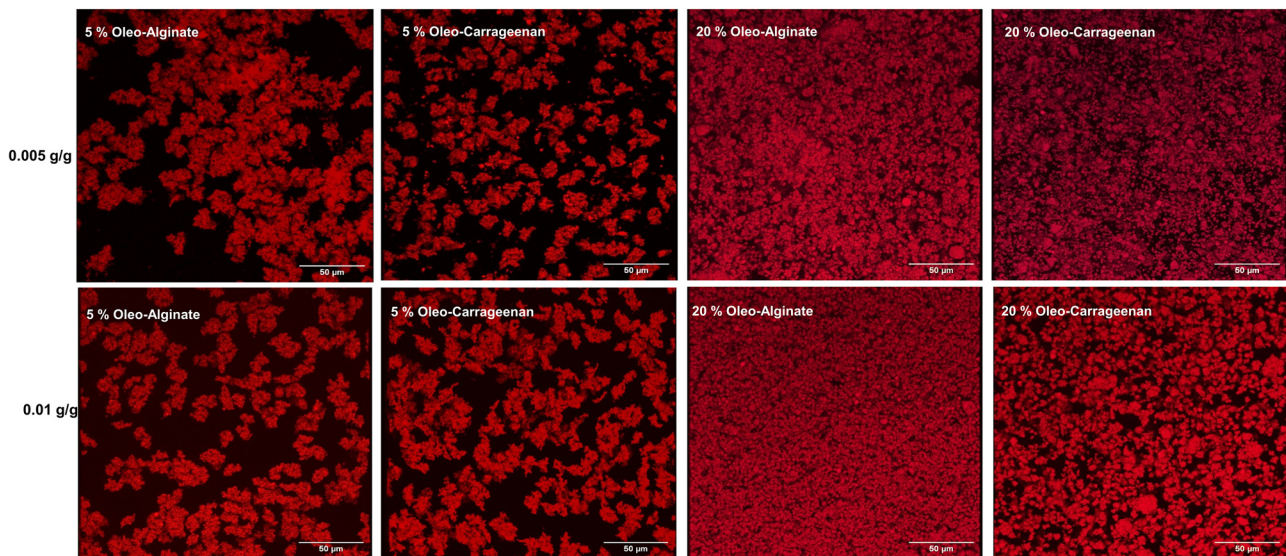


FIG. 12. Confocal laser scanning microscopy (CLSM) images from the different bridging flocculated emulsions with alginate and carrageenan at two fixed ratios, 0.005–0.01 g/g, at two 5% and 20% oleosome content. Scale bar: 50 μ m.

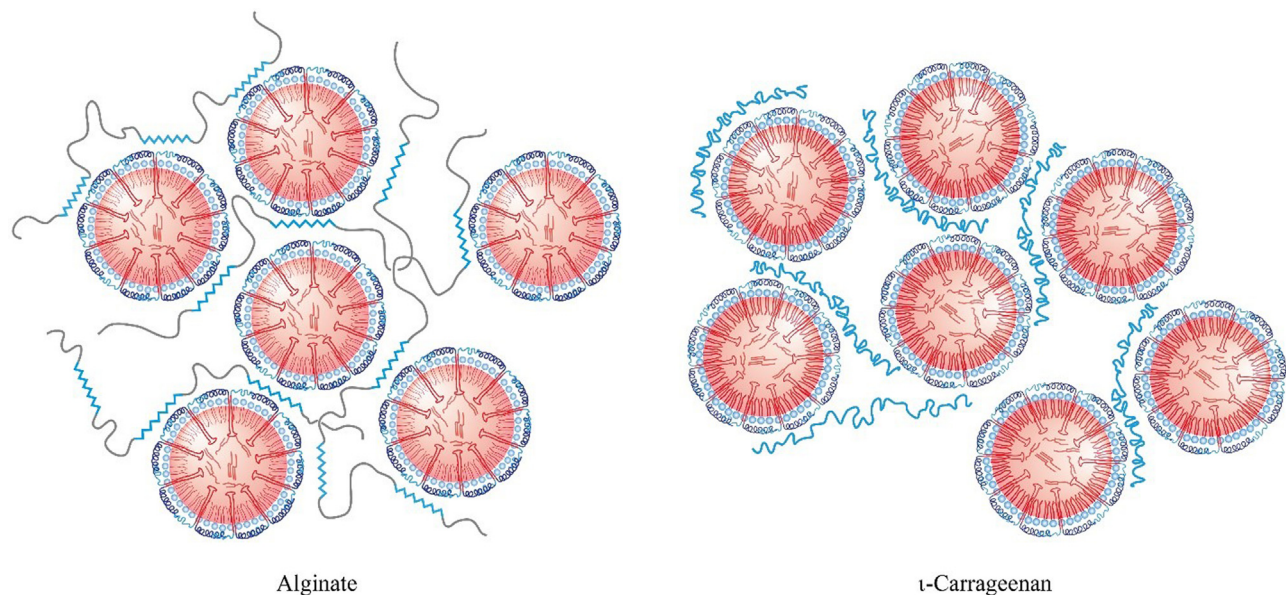


FIG. 13. Schematics of typical oleosome clusters. Alginate binds oleosomes very differently as carrageenan.

Adsorption and bridging of the different hydrocolloids are responsible for the distinct mechanical behavior. This is shown in Fig. 13. Once oleosomes become connected by different chains, a network with embedded oleosomes emerges. The shear modulus is defined roughly by the number of electrostatic connections between charged alginate blocks and oleosomes and the number of entanglements, which contribute as topological constraints (slip-links) to the shear modulus (Edwards and Vilgis, 1986). The flexible parts of alginate chains in between oleosomes define thus a large part of the (entropic) elasticity, very similar to conventional gels, filled with nanoparticles. On the other hand, the negatively charged carrageenan chains bind with more monomers to the positively charged surfaces of the oleosomes. The chain of blobs can easily adjust to the oleosome curvature, making the adsorption of the individual chains on the surface stronger. Carrageenan chains interconnect oleosomes less effectively (Fig. 13) and cannot form entangled conformations. Clusters grow only to limited sizes, as seen in the confocal micrographs Fig. 12 for the concentrations of 5% oleosomes with 0.005 and 0.01 g/g polymer. Whereas alginate forms large interconnected clusters at 0.005 g/g, the carrageenan samples show smaller separated clusters at 0.005 and 0.01 g/g. This is not surprising since carrageenan effectively coats the oleosomes, which prevents the adsorption of inter-oleosome connecting chains. Free, non-connected chains remain unattached and contribute to the bulk (compression) modulus. The flexible chains of alginate can even connect clusters of oleosomes.

The moduli in the linear viscoelastic range (LVR) are of the same order of magnitude (see Fig. 10) for alginate and carrageenan-oleosome mixtures, which are mainly determined by the density of oleosomes and clusters in both cases. However, the differences between the hydrocolloids become more pronounced at larger deformations. The main reason is given by the different arrangements and structures of the clusters. At local scales, the properties of the

hydrocolloids come into play. For an illustration, it is helpful to have a closer view of the cluster distribution in both cases, shown in Fig. 14.

Alginate connects oleosomes into large, percolating clusters of irregular shapes, surrounded by small clusters of similar shapes. Carrageenan also forms (at higher polymer concentrations) larger clusters but with less connectivity. During the LVR, the clusters support shear stresses up to 2%–5% strain for both systems.

At the optimum bridging ratio for alginate, 0.005 g/g, both moduli present a sharp decrease, as observed in the slopes in Table II, which are higher than 0.005 g/g carrageenan slope values. In comparison, at 0.01 g/g, carrageenan presents a steeper moduli decrease than 0.01 g/g alginate, which, as previously observed, corresponds to the optimum bridging ratio for carrageenan. This is shown already in Figs. 6 and 13. This behavior has been observed elsewhere, too (Blijdenstein *et al.*, 2004b; Zhao *et al.*, 2014). Steeper slopes indicate sudden microstructure fracture, typical for bridging flocculated systems that have heterogeneous structures. This is caused by local stresses and strains, which are highest near the weakest links between the oleosomes and allows fractures quickly propagate through the largest clusters. The breaking of the links finally involves the polymers themselves. The shear energy needs to be larger than the electrostatic binding of the charged parts of the polymers at the oleosome surfaces. In the case of carrageenan, this is easier and even reversible. Under shear, some of the oleosomes at the weak links lose some chains, but the dissolved chains quickly coat the free surface. For alginate, the topological, transient network needs to disentangle. Since there is no longer a possibility of rearrangement of the entanglement network, the decay slope is steeper.

IV. CONCLUSION

This study aimed to determine the effect of the type and ratio of polysaccharides on the gelation of soybean oleosomes using a polymer

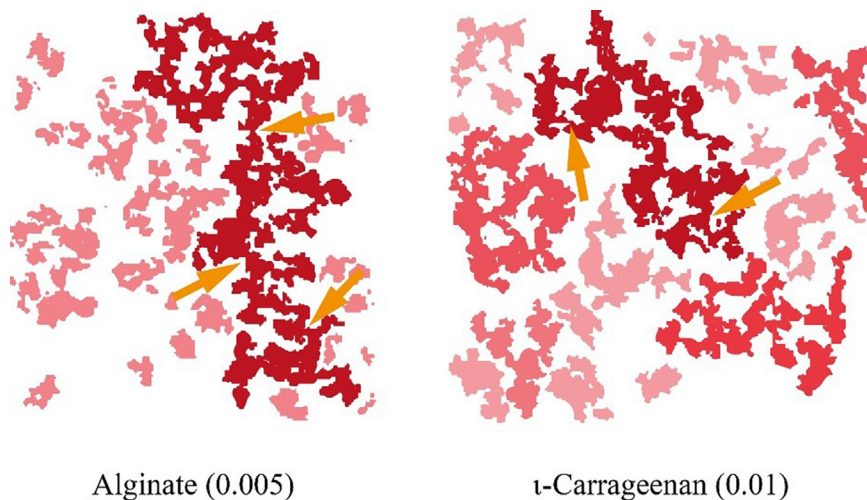


FIG. 14. Comparison of the cluster distribution between the samples containing alginate (at 0.005 g/g) and ι -carrageenan (at 0.01 g/g). The different color intensities indicate as guide to the eye the cluster size. The clusters have been extracted from the corresponding CLSM results, Fig. 11. Representative weak links are indicated by arrows.

bridging mechanism. It was shown that negatively charged polysaccharides with flexible polymer chains, such as sodium alginate and ι -carrageenan, can bridge oleosome droplets, via electrostatic attractions, into a particle gel network. However, structural differences between alginate and carrageenan, such as charge distribution along its backbone, account for differences in adsorption behavior to the oleosome surface. Alginate adsorbs block-wise due to its charged units arranged in blocks along its backbone, whereas carrageenan chains adsorb uniformly due to its uniformly distributed charges. This difference will influence bridging efficiency, where alginate presented greater bridging efficiency (0.4 mg/m^2) than carrageenan (0.8 mg/m^2). Alginate flexible chains allow for more freedom, enabling interconnecting of multiple oleosome droplets into a percolated network.

On the other hand, carrageenan will be more efficient for completely coating the oleosome surface but less efficient for bridging since more charged monomers are adsorbed on the oleosome surface, thus preventing chains from interconnecting further oleosome droplets. This difference in bridging efficiency will influence microstructural properties. Alginate forms more heterogeneous and interconnected clusters, while carrageenan forms smaller and less interconnected clusters. These microstructural differences will influence rheological response upon larger deformations, where steeper slopes in G' ; indicating fracture behavior, are caused by quick stress propagation from weak links within the clusters. Therefore, it is concluded that sodium alginate is an efficient polysaccharide to produce oleogels based on oleosome emulsions via a polymer bridging mechanism.

ACKNOWLEDGMENTS

The authors would like to thank the referees for their constructive and useful criticism. Their helpful comments improved the draft version of the manuscript very much.

AUTHOR DECLARATIONS

Conflict of Interest

The authors have no conflicts to disclose.

Author Contributions

Juan Carlos Zambrano Solorzano: Conceptualization (equal); Data curation (equal); Formal analysis (equal); Investigation (equal); Methodology (equal); Project administration (equal); Resources (equal); Software (equal); Writing – original draft (equal). **Thomas A. Vilgis:** Conceptualization (equal); Formal analysis (equal); Funding acquisition (equal); Project administration (equal); Software (equal); Supervision (equal); Validation (equal); Visualization (equal); Writing – review & editing (equal).

DATA AVAILABILITY

The data that support the findings of this study are available from the corresponding author upon reasonable request.

REFERENCES

- Ahn, Y., Kim, H., and Kwak, S.-Y., "Self-reinforcement of alginate hydrogel via conformational control," *Eur. Polym. J.* **116**, 480–487 (2019).
- Blijdenstein, T., Van Winden, A., Van Vliet, T., Van der Linden, E., and Van Aken, G., "Serum separation and structure of depletion-and bridging-flocculated emulsions: A comparison," *Colloids Surf., A* **245**(1–3), 41–48 (2004a).
- Blijdenstein, T. B., van der Linden, E., van Vliet, T., and van Aken, G. A., "Scaling behavior of delayed demixing, rheology, and microstructure of emulsions flocculated by depletion and bridging," *Langmuir* **20**(26), 11321–11328 (2004b).
- Chang, C.-W. and Liao, Y.-C., "Accelerated sedimentation velocity assessment for nanowires stabilized in a non-Newtonian fluid," *Langmuir* **32**(51), 13620–13626 (2016).
- De Gennes, P.-G., *Scaling Concepts in Polymer Physics* (Cornell University Press, 1979).
- de Wijk, R. A., Janssen, A. M., and Prinz, J. F., "Oral movements and the perception of semi-solid foods," *Physiol. Behav.* **104**(3), 423–428 (2011).
- Dickinson, E., "Strategies to control and inhibit the flocculation of protein-stabilized oil-in-water emulsions," *Food Hydrocolloids* **96**, 209–223 (2019).
- Dickinson, E. and Parkinson, E. L., "Heat-induced aggregation of milk protein-stabilized emulsions: Sensitivity to processing and composition," *Int. Dairy J.* **14**(7), 635–645 (2004).
- Dickinson, E. and Pawlowsky, K., "Effect of high-pressure treatment of protein on the rheology of flocculated emulsions containing protein and polysaccharide," *J. Agric. Food Chem.* **44**(10), 2992–3000 (1996).

- Dickinson, E. and Pawlowsky, K., "Influence of κ -carrageenan on the properties of a protein-stabilized emulsion," *Food Hydrocolloids* **12**(4), 417–423 (1998).
- Diedericks, C. F., De Koning, L., Jideani, V. A., Venema, P., and Van der Linden, E., "Extraction, gelation and microstructure of Bambara groundnut vicilins," *Food Hydrocolloids* **97**, 105226 (2019).
- Dobrynin, A. V., Colby, R. H., and Rubinstein, M., "Scaling theory of polyelectrolyte solutions," *Macromolecules* **28**(6), 1859–1871 (1995).
- Dobrynin, A. V. and Jacobs, M., "When do polyelectrolytes entangle?," *Macromolecules* **54**(4), 1859–1869 (2021).
- Doi, M. and Edwards, S. F., *The Theory of Polymer Dynamics* (Oxford University Press, 1988), Vol. 73.
- Edwards, S. and Vilgis, T., "The effect of entanglements in rubber elasticity," *Polymer* **27**(4), 483–492 (1986).
- Fuhrmann, P. L., Sala, G., Scholten, E., and Stieger, M., "Influence of clustering of protein-stabilised oil droplets with proanthocyanidins on mechanical, tribological and sensory properties of o/w emulsions and emulsion-filled gels," *Food Hydrocolloids* **105**, 105856 (2020).
- Fuhrmann, P. L., Sala, G., Stieger, M., and Scholten, E., "Clustering of oil droplets in o/w emulsions: Controlling cluster size and interaction strength," *Food Res. Int.* **122**, 537–547 (2019).
- Grant, M. and Russel, W., "Volume-fraction dependence of elastic moduli and transition temperatures for colloidal silica gels," *Phys. Rev. E* **47**(4), 2606 (1993).
- Huang, A. H., "Oil bodies and oleosins in seeds," *Annu. Rev. Plant Physiol. Plant Mol. Biol.* **43**(1), 177–200 (1992).
- Kanai, H., Navarrete, R., Macosko, C., and Scriven, L., "Fragile networks and rheology of concentrated suspensions," *Rheol. Acta* **31**(4), 333–344 (1992).
- Kantor, Y. and Webman, I., "Elastic properties of random percolating systems," *Phys. Rev. Lett.* **52**(21), 1891 (1984).
- Lee, H. A., Choi, S. J., and Moon, T. W., "Characteristics of sodium caseinate- and soy protein isolate-stabilized emulsion-gels formed by microbial transglutaminase," *J. Food Sci.* **71**(6), C352–C357 (2006).
- Lips, A., Campbell, I., and Pelan, E., "Aggregation mechanisms in food colloids and the role of biopolymers," in *Food Polymers, Gels and Colloids* (Elsevier, 1991), pp. 1–21.
- Mao, Y. and McClements, D. J., "Modulation of emulsion rheology through electrostatic heteroaggregation of oppositely charged lipid droplets: Influence of particle size and emulsifier content," *J. Colloid Interface Sci.* **380**(1), 60–66 (2012).
- Matsumoto, A., Zhang, C., Scheffold, F., and Shen, A. Q., "Microrheological approach for probing the entanglement properties of polyelectrolyte solutions," *ACS Macro Lett.* **11**(1), 84–90 (2021).
- Mellema, M., Van Opheusden, J., and Van Vliet, T., "Categorization of rheological scaling models for particle gels applied to casein gels," *J. Rheol.* **46**(1), 11–29 (2002).
- Nie, H., He, A., Zheng, J., Xu, S., Li, J., and Han, C. C., "Effects of chain conformation and entanglement on the electrospinning of pure alginate," *Biomacromolecules* **9**(5), 1362–1365 (2008).
- Patel, A., Longmore, N., Mohanan, A., and Ghosh, S., "Salt and pH-induced attractive interactions on the rheology of food protein-stabilized nano-emulsions," *ACS Omega* **4**(7), 11791–11800 (2019).
- Roulet, M., Clegg, P. S., and Frith, W. J., "Rheology of protein-stabilised emulsion gels envisioned as composite networks. 2-framework for the study of emulsion gels," *J. Colloid Interface Sci.* **594**, 92–100 (2021).
- Sahimi, M. and Arbabi, S., "Mechanics of disordered solids. II. Percolation on elastic networks with bond-bending forces," *Phys. Rev. B* **47**(2), 703 (1993).
- Segre, P., Prasad, V., Schofield, A. B., and Weitz, D., "Glasslike kinetic arrest at the colloidal-gelation transition," *Phys. Rev. Lett.* **86**(26), 6042 (2001).
- Trappe, V. and Weitz, D., "Scaling of the viscoelasticity of weakly attractive particles," *Phys. Rev. Lett.* **85**(2), 449 (2000).
- Tzen, J. T., Cao, Y., Laurent, P., Ratnayake, C., and Huang, A. H., "Lipids, proteins, and structure of seed oil bodies from diverse species," *Plant Physiol.* **101**(1), 267–276 (1993).
- Upadhyay, R., Aktar, T., and Chen, J., "Perception of creaminess in foods," *J. Texture Stud.* **51**(3), 375–388 (2020).
- van der Linden, E. and Sagis, L. M., "Isotropic force percolation in protein gels," *Langmuir* **17**(19), 5821–5824 (2001).
- Veerman, C., de Schiffart, G., Sagis, L. M., and van der Linden, E., "Irreversible self-assembly of ovalbumin into fibrils and the resulting network rheology," *Int. J. Biol. Macromol.* **33**(1–3), 121–127 (2003).
- Veerman, C., Ruis, H., Sagis, L. M., and van der Linden, E., "Effect of electrostatic interactions on the percolation concentration of fibrillar β -lactoglobulin gels," *Biomacromolecules* **3**(4), 869–873 (2002).
- Vilgis, T. A., "Texture, taste and aroma: Multi-scale materials and the gastrophysics of food," *Flavour* **2**(1), 1–5 (2013).
- Wang, X., Li, X., Xu, D., Zhu, Y., Cao, Y., Li, X., and Sun, B., "Modulation of stability, rheological properties, and microstructure of heteroaggregated emulsion: Influence of oil content," *LWT* **109**, 457–466 (2019).
- Waschatko, G., Schiedt, B., Vilgis, T. A., and Junghans, A., "Soybean oleosomes behavior at the air–water interface," *J. Phys. Chem. B* **116**(35), 10832–10841 (2012).
- Wu, N.-N., Yang, X.-Q., Teng, Z., Yin, S.-W., Zhu, J.-H., and Qi, J.-R., "Stabilization of soybean oil body emulsions using κ , ι , λ -carrageenan at different pH values," *Food Res. Int.* **44**(4), 1059–1068 (2011).
- Xi, Z., Liu, W., McClements, D. J., and Zou, L., "Rheological, structural, and microstructural properties of ethanol induced cold-set whey protein emulsion gels: Effect of oil content," *Food Chem.* **291**, 22–29 (2019).
- Zambrano, J. C. and Vilgis, T. A., "Tunable oleosome-based oleogels: Influence of polysaccharide type for polymer bridging-based structuring," *Food Hydrocolloids* **137**, 108399 (2023).
- Zhai, H., Gunness, P., and Gidley, M. J., "Depletion and bridging flocculation of oil droplets in the presence of β -glucan, arabinoxylan and pectin polymers: Effects on lipolysis," *Carbohydr. Polym.* **255**, 117491 (2021).
- Zhao, C., Yuan, G., and Han, C. C., "Bridging and caging in mixed suspensions of microspheres and adsorptive microgel," *Soft Matter* **10**(44), 8905–8912 (2014).
- Zhao, C., Yuan, G., Jia, D., and Han, C. C., "Macrogel induced by microgel: Bridging and depletion mechanisms," *Soft Matter* **8**(26), 7036–7043 (2012).